ELSEVIER

Contents lists available at ScienceDirect

BBA - Biomembranes

journal homepage: www.elsevier.com/locate/bbamem



The antioxidant vitamin E as a membrane raft modulator: Tocopherols do not abolish lipid domains



Mitchell DiPasquale^a, Michael H.L. Nguyen^a, Brett W. Rickeard^a, Nicole Cesca^a, Christopher Tannous^a, Stuart R. Castillo^a, John Katsaras^{b,c,d}, Elizabeth G. Kelley^e, Frederick A. Heberle^f. Drew Marquardt^{a,g,*}

- ^a Department of Chemistry and Biochemistry, University of Windsor, Windsor, Ontario, Canada
- ^b Neutron Scattering Division, Oak Ridge National Laboratory, Oak Ridge, TN 37831, USA
- ^c Joint Institute for Neutron Sciences, Oak Ridge National Laboratory, Oak Ridge, TN 37831, USA
- ^d Department of Physics and Astronomy, University of Tennessee, Knoxville, TN 37996, USA
- ^e NIST Center for Neutron Research, National Institute of Standards and Technology, Gaithersburg, MD, USA
- f Department of Chemistry, University of Tennessee, Knoxville, TN 37996, USA
- g Department of Physics, University of Windsor, Windsor, Ontario, Canada

ARTICLE INFO

Keywords: Vitamin E α -Tocopherol γ -Tocopherol Lipid rafts Small-angle neutron scattering Lipid bilayer

ABSTRACT

The antioxidant vitamin E is a commonly used vitamin supplement. Although the multi-billion dollar vitamin and nutritional supplement industry encourages the use of vitamin E, there is very little evidence supporting its actual health benefits. Moreover, vitamin E is now marketed as a lipid raft destabilizing anti-cancer agent, in addition to its antioxidant behaviour. Here, we studied the influence of vitamin E and some of its vitamers on membrane raft stability using phase separating unilamellar lipid vesicles in conjunction with small-angle scattering techniques and fluorescence microscopy. We find that lipid phase behaviour remains unperturbed well beyond physiological concentrations of vitamin E (up to a mole fraction of 0.10). Our results are consistent with a proposed line active role of vitamin E at the domain boundary. We discuss the implications of these findings as they pertain to lipid raft modification in native membranes, and propose a new hypothesis for the antioxidant mechanism of vitamin E.

1. Introduction

Vitamin E was discovered in 1922 by Evans and Bishop as a vital dietary biomolecule for mammalian reproduction [1]. Yet, to this day its precise biological role continues to be debated [2,3,4]. Vitamin E refers to two families of molecules known as tocopherols and tocotrienols, each comprised of four members (α , β , γ , and δ) differing in the methylation of their chromanol ring (see Fig. 1). Considering this somewhat minor structural difference between family members, and the fact that all species are regularly consumed in the average diet, it is remarkable that α -tocopherol is the only one of the eight variants actively retained by the human body [5,6].

A large body of literature advocates that vitamin E is the first line of defense for cell membranes against oxidation [8,9]. As a result, vitamin E is commonly used as a bio-compatible preservative in the cosmetic and food industries [7]. However, and to the best of our knowledge, the role of vitamin E *in vivo* remains ambiguous. Some studies allude to a

role in homeostatic processes, and deficiency of vitamin E leads to diseases such as infertility and neuromuscular dysfunction, all without elucidated mechanisms [1,10]. The lack of good experimental evidence and the fact that vitamin E is found in extremely low concentrations *in vivo* [11], call into question its antioxidant-centric role [4].

It is not surprising that vitamin E properties are propagated by industry and health professionals that advocate for the sale of dietary supplements. Across North America, an estimated sixty percent of middle-to-late-aged adults consume vitamins, including vitamin E, while sufficient recommended amounts can generally be obtained from a balanced diet [12]. Nutrition companies offer a variety of vitamin E supplements ranging from pure RRR- α -tocopherol to "natural" mixtures containing all of the tocopherol family members, often in amounts ranging from 3 to 30 times the recommended daily intake [7]. While the health benefits of sufficient dietary antioxidants are well documented, vitamin E is also marketed for promoting cardiovascular health and as an anti-cancer agent [13,14].

E-mail address: drew.marquardt@uwindsor.ca (D. Marquardt).

^{*} Corresponding author.

<u>Structure</u>	R_1	R_2	S
α-tocopherol (αToc)	CH ₃	CH ₃	γ
β-tocopherol	CH ₃	Н	δ

 α -tocopherol quinone (α TocQ)

Structure	\mathbf{R}_{1}	$\mathbf{R_2}$
γ-tocopherol (γToc)	Н	CH ₃
δ-tocopherol	Н	Н

Fig. 1. Structures of different tocopherols, specifically: α -tocopherol (α Toc) the species preferentially taken-up by the human body; γ -tocopherol (γ Toc) the most naturally abundant species [7]; and the stable oxidation product of α Toc, α -tocopherylquinone (α TocQ).

The rationale for vitamin E as an anti-cancer agent is predicated on a proposed mechanism of membrane raft destabilization [15]. Cell membranes have been implicated in a vast array of cellular processes, which can often be facilitated by the lateral organization of lipids and proteins into micro and nanoscale "rafts" [16,17]. It is thought that certain varieties of cancer cells, particularly prostate and breast, possess more robust lipid rafts that can be destabilized through cholesterol depletion by raft-modulating agents such as methyl- β -cyclodextrin [18,15,19]. This hypothesis has thus inspired many studies investigating the potential anti-cancer effects of vitamin E. Notably, Yang et al. have suggested that high-dose supplementation of γ - and δ - to-copherols inhibits tumorigenesis, while α -tocopherol does not [20,21,22]. Conversely, clinical trials involving α -tocopherol supplementation indicate an increased risk for developing prostate cancer in healthy men [14,13].

Observations of membrane rafts have been elusive in live cells, presumably due to their proposed small size and transient nature, in addition to the inherent complexity of biological membranes [23,24]. More recently, lipid domains on the order of 40 nm in size were observed in living bacteria [25]. Three-component lipid mixtures mimicking the outer leaflet of eukaryotic plasma membranes are commonly used as model systems for the study of lipid rafts [26,27]. Specifically, vesicles composed of high- and low-melting lipids, and cholesterol are thermodynamically unstable and demix into a cholesterol-rich liquid ordered (L_o) phase that coexists with a cholesterol-poor liquid disordered (L_d) phase. These structures are compatible for study by a range of biophysical techniques, including small-angle neutron and X-ray scattering [28], and fluorescence microscopy [29,30,31].

In the current study we looked at how vitamin E affects lipid membranes, and if its behaviour is consistent with raft-disrupting anticancer mechanisms, in the hope of gaining a better understanding of vitamin E supplementation.

2. Materials and methods

2.1. Materials

1,2-Dipalmitoyl-sn-glycero- 3-phosphocholine (16:0/16:0 PC, DPPC), 1,2-dipalmitoyl-d62-sn-glycero-3-phosphocholine (16:0[d31]/16:0[d31] PC, d62-DPPC), 1,2-dioleoyl-sn-glycero-3-phosphocholine (18:1/18:1 PC, DOPC), and 1,2-dipalmitoyl-sn-glycero-3-phosphoethanolamine-N-

(lissamine rhodamine B sulfonyl) (LR-DPPE) were purchased from Avanti Polar Lipids, Inc. (Alabaster, AL). Cholesterol, DL-all-rac- α -tocopherol (α -tocopherol, α Toc), (R,R,R)- γ -tocopherol (γ -tocopherol, γ Toc), D- α -tocopherylquinone (α -tocopherylquinone, α TocQ), and sucrose were purchased from Sigma-Aldrich (St. Louis, MO). Naphtho-[2,3-a]pyrene (naphthopyrene) was purchased from TCI America (Tokyo, Japan). 99.9% D₂O was purchased from Cambridge Isotopes (Andover, MA). All reagents were used without further purification.

2.2. SANS sample preparation

2.2.1. Selection of lipid composition

All experiments were performed using a mixture of DPPC/DOPC/Chol at a mole ratio of 37.5/37.5/25, respectively. This composition contains a 1:1 ratio of high- and low-melting lipids such that the area fractions of L_o phase and L_d phase domains are approximately equal. The phase behaviour of this composition has carefully been characterized by different techniques in a number of previous studies, thereby offering a reliable membrane platform for this work [30,32,33].

2.2.2. Preparation of unilamellar vesicles

Well-established protocols were followed to prepare unilamellar vesicles (ULVs) for scattering measurements. In brief, lipid mixtures were prepared by transferring desired volumes of stock solutions in HPLC-grade chloroform to a scintillation vial using a glass syringe (Hamilton, Reno, NV, USA). Lipid films were formed through chloroform evaporation under a gentle argon stream, followed by trace solvent removal in vacuo for > 12 h. The films were hydrated to 20 mg/ml by the addition of a 34.6% D₂O/H₂O mixture, and incubated for 30 min at 50 °C prior to the formation of a multilamellar vesicle (MLV) suspension by vortexing. The ratio of D₂O/H₂O was used to replicate the contrast matching scheme described by Heberle et al., such that the scattering length density of the aqueous solvent is simultaneously matched to that of the lipid headgroup and average hydrocarbon chain compositions. This contrast matching scheme minimizes scattering contributions arising from transverse (i.e., normal to the plane of the bilayer) scattering length density variation, and emphasizes scattering contributions arising from in-plane heterogeneity (i.e., demixing of lipids with saturated and unsaturated chains) [34]. The MLV suspension was subjected to 5 freeze/thaw cycles between -80° C and 50 °C, followed by vortexing at 50 °C. ULVs were then prepared by 31 passes through a hand-held miniextruder equipped with a 50 nm pore-diameter polycarbonate filter (Avanti Polar Lipids, Alabaster, AL) and heated to 50 °C. Extruded vesicles were characterized by dynamic light scattering using a Malvern ZetaSizer Nano ZS (Malvern Panalytical, Ltd., Malvern, UK).

2.3. Characterization of phase separation by contrast-matched SANS

Neutron scattering experiments were performed at the Very Small-Angle Neutron Scattering (NG3-VSANS) instrument located at the National Institute of Standards and Technology Center for Neutron Research (NIST-CNR). The white beam option was configured to use a neutron wavelength of 5.3 Å with a $\Delta\lambda/\lambda$ of 40%. Data were collected using two detector carriages positioned at sample-to-detector distances of 5.4 m and 13 m. This large wavelength spread results in lower qresolution, but allows for a higher neutron flux at the sample, and thus shorter count times. In this case, good quality data in the scattering vector range of 0.009 Å $^{-1}$ < q < 0.5 Å $^{-1}$ were acquired in three minutes.

Additional experiments were performed at the CG-3 Bio-SANS instrument of the High Flux Isotope Reactor (HFIR) located at Oak Ridge National Laboratory (ORNL). Data were taken at a sample-to-detector distance of 15.5 m using 6 Å wavelength neutrons (fwhm 15%). A total scattering vector of 0.003 Å $^{-1}$ < q < 0.8 Å $^{-1}$ was collected using a two-dimensional (1 m \times 1 m) 3 He position-sensitive detector

(ORDELA, Inc., Oak Ridge, TN) with 192 \times 256 pixels in combination with a 1 m \times 0.8 m wing detector that comprised 160 \times 256 pixels and rotated by 1.40°.

ULV suspensions of 20 mg/ml were loaded into 1 mm path-length banjo cells (Hellma USA, Plainview, NY) and mounted in a Peltier temperature-controlled cell holder with $\approx 1\,^{\circ}\text{C}$ accuracy. Samples were measured at 7 temperatures, ranging from the two-phase (Lo / Ld) liquid coexistence regime at lower temperatures through to the uniformly melted Ld phase at higher temperatures. At a minimum, samples were permitted to equilibrate at each temperature for 20 min prior to measurement. Data were reduced, stitched, and corrected for detector pixel sensitivity, dark current, sample transmission, and background scattering from water using ORNL's Mantid software (BioSANS) [35] or the appropriate Igor Pro macros (VSANS) provided by NIST-CNR [36].

The resulting data were analyzed in a model-independent manner using the Porod invariant to represent the total scattering intensity [37]:

$$Q = \int_{0}^{\infty} q^{2}I(q)dq \tag{1}$$

With the contrast matching scheme used here, to a first approximation, Q is only dependent on the area fraction of the L_o phase (a_{L_o}) and the difference in contrast between the L_o and L_d domains $(\Delta \rho)$ [38]:

$$Q \approx a_{L_0} (1 - a_{L_0}) \Delta \rho^2 \tag{2}$$

Since neutron contrast depends on how strongly the deuterated and protiated lipids are segregated, SANS measurements can detect changes in domain area fraction (a_{L_0}) or a change in the partitioning of the lipids between the coexisting phases. For example, either a decrease in domain area fraction, or reduced partitioning of saturated and unsaturated lipids between the two phases, will cause a decrease in the total scattering according to Eq. (2). Both of these features imply a destabilization of lipid domains.

2.4. Bilayer structure from SAXS

Small angle X-ray scattering (SAXS) experiments were performed on the same samples measured by SANS. ULVs at a concentration of 10 mg/ml were measured using a Rigaku BioSAXS-2000 (Rigaku Americas, The Woodlands, TX) equipped with a Pilatus 100 K detector and an HF007 rotating copper anode source. All samples were measured above the phase transition temperature (50 °C) to ensure well mixed bilayers. Multiple measurements were obtained for each sample, and samples were monitored for radiation damage before averaging. Resulting form factors in the scattering vector range of 0.04 Å $^{-1}$ < q < 0.6 Å $^{-1}$ were background-corrected using PRIMUS [39] and modelled using the Global Analysis Program (GAP) developed by Pabst et al. [40,41].

2.5. Preparation and fluorescence imaging of giant unilamellar vesicles

Giant unilamellar vesicles (GUVs) suitable for epifluorescence microscopy were generated using a modified electroformation protocol as described by Konyakhina and Feigenson [42,43]. In brief, lipid mixtures with and without a vitamin E mole fraction of 0.10 ($\chi=0.10$) were mixed in chloroform and combined with fluorescent probes at predefined mole ratios. The mixture was then spread evenly onto a conductive indium tin oxide (ITO)-coated slide (Delta Technologies, LTD., Loveland, CO). The fluorescent probes ($\chi_{LR-DPPE}=0.005$ and $\chi_{naphthopyrene}=0.01$) were chosen based on their known lipid phase partitioning behaviour [44]. Solvent was removed by overnight drying in vacuo for > 12 h. GUVs were then formed in 100 mmol/L aqueous sucrose by heating for 1 h at 50 °C with electroformation by a 10 Hz sinusoidal current with a peak-to-peak amplitude of 1 V. The samples were gradually cooled to room temperature over 10 h using a Digi-

Sense benchtop temperature controller (Cole Parmer, Vernon Hills, IL) to minimize kinetically-trapped domain artifacts. GUVs were transferred to a glass coverslip enclosed by a silicon gasket, sealed by a glass slide, and allowed to settle for 1 h prior to imaging. All samples were imaged at ambient temperature within 24 h of preparation using an inverted epifluorescence microscope (Leica DMI6000, Wetzlar, Germany). LR-DPPE was detected using a Texas Red filter cube (ex. 594 nm/em. 598 nm) and naphthopyrene was detected using a DAPI filter cube (ex. 357 nm/em. 459 nm). Care was taken to prevent light-induced phase separation by minimizing illumination intensity and exposure [45,46]. Resulting images were artificially recoloured for publication using the Leica LAS X software to improve accessibility for readers with vision impairment.

3. Results and discussion

3.1. Tocopherol does not affect bilayer structure

Phase separating ULVs suspended in water were heated to 50 °C to ensure a uniform distribution of the lipids, thus ensuring a bilayer of uniform thickness suitable for structural studies by SAXS. To quantify any differences in bilayer structure, the scattering form factors were modelled using the GAP program to determine physical parameters [40,41]. GAP models an electron density profile of the bilayer by parameterizing three Gaussians, one for each electron-rich head group and one for the hydrocarbon region. As X-rays are sensitive to the electron-rich phosphates in the lipid head groups, we report the head-group-headgroup distance of the bilayers (d_{HH}) from the optimized modelled form factor. Note, d_{HH} is directly determined and requires no subsequent calculations or assumptions about the system. As explained in the SI, due to the complexity of the multi-component systems, some parameters were fixed to refine the fit.

Table 1 summarizes d_{HH} for each composition studied and additional fit parameters are shown in Table S1 of the Supplementary Material. Measured headgroup-headgroup distances for DPPC/DOPC/Chol are consistently within 2% of previously reported values [33,47,48]. Interestingly, up to a mole fraction of 10% tocopherol, the transverse bilayer structure is not significantly perturbed. The slight thinning of the bilayer upon addition of tocopherol is likely an artifact of fixing the width of the Gaussian describing the headgroup, σ H. Due to the orientation of tocopherol in the membrane, with its chromanol headgroup residing at the hydrophilic interface [49,50,51], additional electron density will be present slightly inside the headgroup Gaussian, which is best described by a wider σ H and an asymmetric Gaussian. Since the GAP program cannot parameterize for skewed Gaussians, it

Table 1Bilayer thickness, represented by the headgroup-headgroup distance, D_{HH}, as a function of percent tocopherol. Parameters were derived from modelling small angle X-ray scattering data, with uncertainties defined as 2%.

Composition	D_{HH} (Å)
DPPC/DOPC/Chol	39.9 ± 0.8
+ 2 % αToc	39.2 ± 0.8
+ 5 % αToc	39.2 ± 0.8
+ 2 % γToc	39.7 ± 0.8
+ 10 % γToc	39.2 ± 0.8
+ 2 % αTocQ	39.1 ± 0.8
+ 10 % αTocQ	38.5 ± 0.8

The following parameters were fixed based on physical considerations as described in the SI [47]: width of Gaussian describing the phosphatidylcholine headgroup, $\sigma H = 3.0$ Å, and amplitude of the Gaussian describing the hydrocarbon tail, relative to that of the headgroup, $\rho C = -1.0$. All fit parameters are tabulated in Table S1.

compensates for this distribution by shifting the position of the head-group, zH, closer to the bilayer center. This trend is most dramatic for $\alpha TocQ$, though only 1.4 Å thinner, where the electron-rich benzoquinone head contributes to a greater proportion of the electron density within the bilayer, just beyond the phosphate group. Indirectly, this suggests that both γToc and $\alpha TocQ$ are likely to localize in the membrane similarly to αToc , consistent with past neutron diffraction observations [51].

3.2. Tocopherol destabilises microscopic phase separation

GUVs are widely used as models for probing the existence and morphology of phase separation at the microscopic level. In this study, the DPPC/DOPC/Chol (37.5/37.5/25) system displays robust

hemispherical domains that can be visualized by the selective partitioning of naphthopyrene and LR-DPPE into the L_o and L_d membrane environments, respectively (Fig. 2A) [44]. At ambient temperature, the addition of $\chi=0.10~\alpha$ - (Fig. 2B) or γ -tocopherol(Fig. 2C) appears to abolish the phase separation, although the presence of domains smaller than the optical resolution limit ($\approx 200~\text{nm}$) cannot be ruled out. Similar suppression of phase separation is observed by heating the system to a point where the mixing entropy, which favours the random arrangement of lipids, dominates over the non-ideal enthalpic contribution to free energy, and results in increased acyl chain disorder and increased lateral lipid diffusion.

In contrast to α - and γ -tocopherol, the presence of α -tocopherylquinone (α TocQ), even up to a mole fraction of 0.10, does not appear to change the phase behaviour (Fig. 2D).

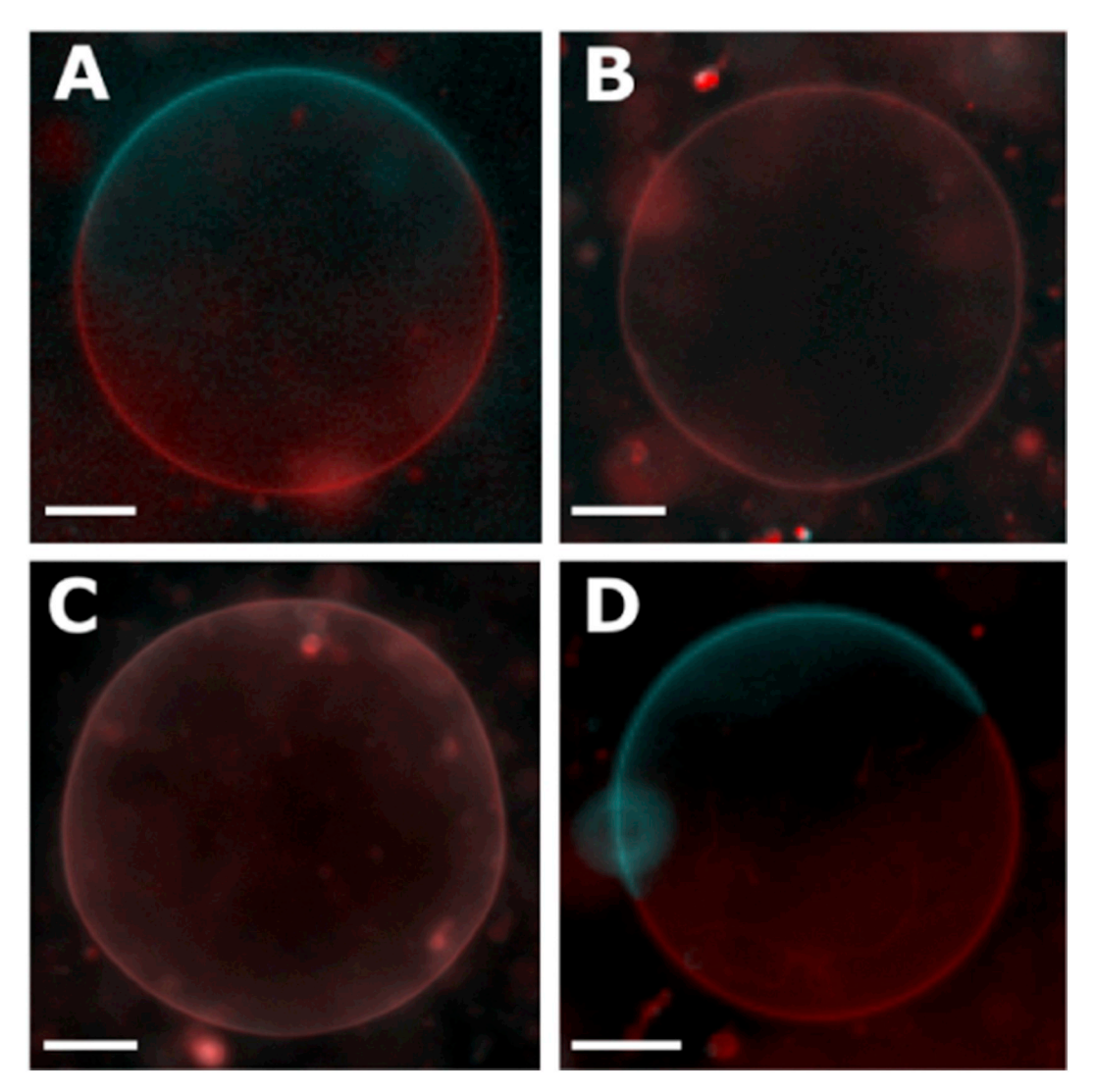


Fig. 2. Fluorescence microscopy of GUVs composed of (A) DPPC/DOPC/Chol; (B) + χ = 0.10 α Toc; (C) + χ = 0.10 γ Toc and (D) + χ = 0.10 α TocQ. Naphthopyrene (blue) preferentially localizes in the L_o phase and LR-DPPE (red) in the L_d phase. Subsequent acquisitions of each fluorophore are colour-merged to highlight the different phases. Phase separation is observed in the undoped system (A) and in the presence of α TocQ (D), but is not observed with α Toc (B) or γ Toc (C).Temperature = 21 °C. Scale bar = 25 μm.

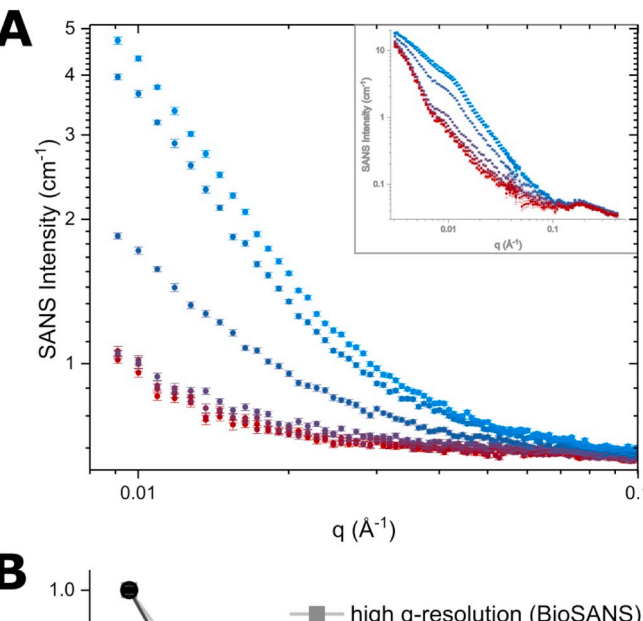
3.3. Domain perturbations described by SANS

Contrast-matched SANS is a powerful tool to probe the lateral organization of lipids within the bilayer and from SANS data one is able to extract precise structural features. An example of this is provided by the modelling of SANS data to determine domain size in refs [34,52]. According to the work of Pencer et al., due to the dependence of the scattering function on contrast, lateral segregation of deuterated and protiated lipids into domains yields a scattering contribution that directly correlates to the extent of phase separation. With this experimental design, data can be reduced to a model-independent scalar quantity known as the Porod invariant, Q (Eq. (2)) representing the total scattering arising from the system's contrast [38]. Using this approach, phase behaviour can easily be obtained from the low q-resolution scattering of laterally heterogeneous vesicles. The DPPC/ DOPC/Chol system (Fig. 3 (A)) shows the difference in scattering obtained by varying the q-resolution. High q-resolution data were collected at CG3-BioSANS (HFIR, ORNL) and low q-resolution data at NG3-VSANS (NCNR). By extracting the Porod invariant and normalizing to a relative scale bound by the highest contrast (lowest temperature) and lowest contrast (highest temperature) data, the temperature dependence of phase separation between samples can be directly compared (Fig. 3B). From this normalized scattering intensity, Qnorm, it can be shown that the decay in scattering intensity is not dependent on q-resolution. The low and high q-resolution data were obtained from different sample preparations of the same composition, and differences in samples may account for the small variations in decay at 25 °C. The low q-resolution "white beam" of VSANS allows for rapid data collection resulting in high sample throughput. However, due to the large wavelength spread, $\frac{\Delta\lambda}{\lambda}$, structural features are lost, as demonstrated by comparing Fig. 3 (A) and the inset to Fig. 3 (A). As a result, modelling the domain size in a fashion similar to Bolmatov et al. is not a viable approach [53]. Nevertheless, the use of the VSANS' "white beam" option provides a 4× increase in flux over conventional SANS experiments and is particularly useful for measuring labile samples that may change during the data acquisition time required to collect good quality data on a conventional SANS instrument.

Low q-resolution SANS curves featured in Fig. 4 show a decrease in scattering intensity as a function of increasing temperature. Phase separation in samples wasconfirmed to be thermodynamically stable and free of hysteresis effects by measuring sequential heating and cooling scans (Fig. S2).

The decrease in scattering intensity is a result of reduced contrast between the lipid phases as they become more miscible, induced by increasing temperature and the addition of tocopherol. Phase separation has been proposed to have biological implications, particularly at the level of protein regulation [54,55]. Though we must be cautious in extrapolating results from vesicle models to biology, this result may suggest that less distinction in the properties of the two phases may diminish the efficacy of segregating membrane proteins solely on the basis of phase preference.

While valuable, the SANS form factors (Fig. 4) do not offer a clear comparison between the different lipid compositions. By reducing the data to Q and normalizing each sample with the bounds of the DPPC/DOPC/Chol system in the absence of tocopherol, we are able to directly compare changes to the membrane by the presence of tocopherol. These trends are shown in Fig. 5 and represents the structurally-independent total scattering from domains as a function of temperature. Remarkably, there is little appreciable deviation in total scattering from samples containing $\chi = 0.02$ or $\chi = 0.05$ α Toc or γ Toc however,



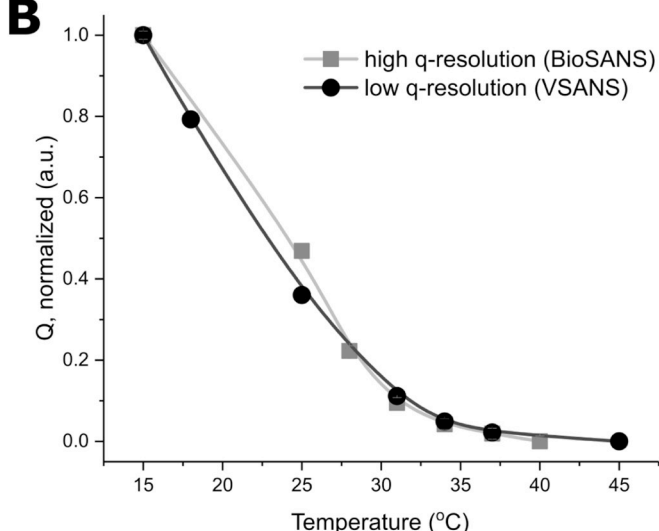


Fig. 3. Comparison of different q-resolution SANS data. (A) Low resolution scattering from DPPC/DOPC/Chol as a function of temperature from 15 °C (blue) to 45 °C (red). The inset shows high q-resolution data from the same sample composition. A logarithmic scale is used to emphasize the difference between the form factors. (B) Normalized scattering intensity (Q) as a function of temperature extracted from both the low- (black circles) and high-resolution (grey squares) data. Error is defined as one standard deviation and the error bars are smaller than the data markers.

domains appear to destabilize at higher ($\chi=0.10$) concentrations. Moreover, due to the strong similarity between the effects of αToc and γToc on phase behaviour, we suggest that this is likely not a determinant in biological selectivity for αToc .

It is noteworthy that even at a high tocopherol concentrations, Q is not totally abolished, indicating that the membrane may not be homogeneous, but still contains nanoscale lateral heterogeneities. More likely, however, residual scattering intensity is a remnant of the inability to contrast match contributions from both lateral and transverse contrast simultaneously.

There are many proposed mechanisms of nanodomain stabilization,

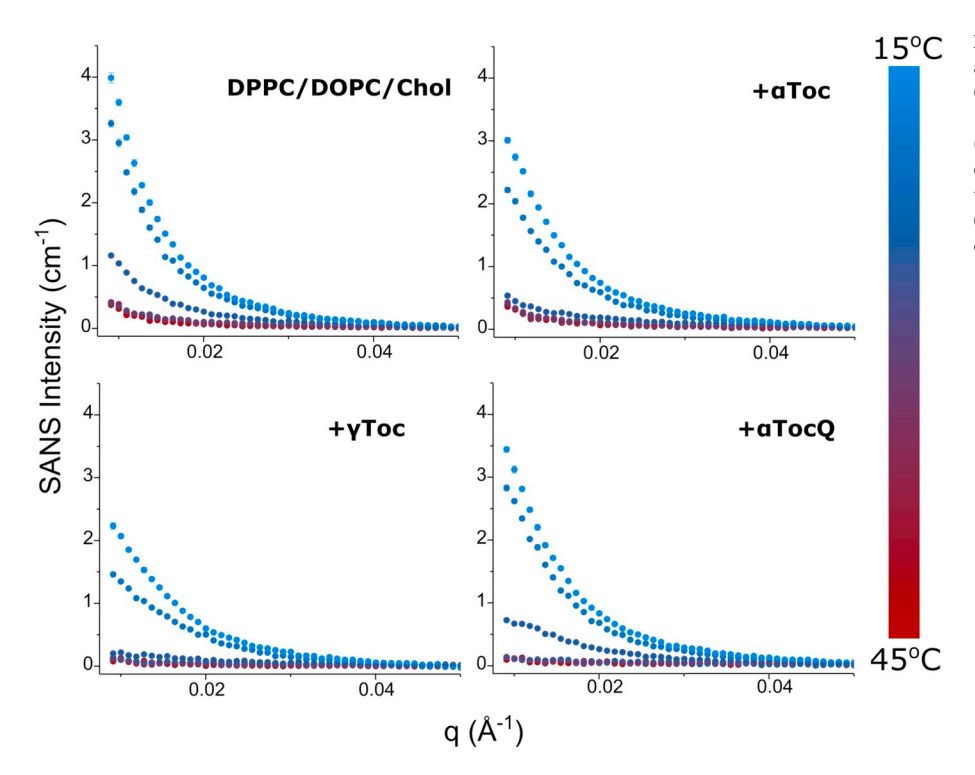


Fig. 4. SANS intensity as a function of temperature and membrane composition. ULVs of DPPC/DOPC/Chol and DPPC/DOPC/Chol + α Toc, + γ Toc, and + α TocQ at a mole fraction of 0.10 were measured at (15, 18, 25, 31, 34, 37, and 45) °C. The presence of different tocopherols modulates both scattering intensity and the rate of intensity decay. Plots show 0.009 Å $^{-1}$ < q < 0.05 Å $^{-1}$ to highlight the difference in scattering at low q.

including coupling of bilayer composition and curvature inducing a microemulsion [56], line tension competing with a long range repulsive force [57], or Ising-like critical fluctuations [58]. Our data do not allow us to discriminate between these or other proposed theories of nanodomain stabilization. The most recently reported mechanism that has been suggested for vitamin E is that of a linactant-induced microemulsion [34,59,60,61].

Muddana et al. previously explored the phase activity of α Toc using coarse-grained Molecular Dynamics simulations to complement GUV microscopy observations [60]. Their results indicate α Toc localizes at the domain interface, thereby acting as a linactant to destabilize macrodomains. We must stress that with SANS we cannot comment on the localization of individual molecules, and though we cannot directly lend support to the mechanism proposed by Muddana et al., our results are qualitatively consistent. In fact, one cannot claim for certain a linactant mechanism without verifying that the molecule preferentially localizes at the phase boundary. Our DPPC/DOPC/Chol system is classified as a Type II phase-separating mixture, which produces macroscopic hemispherical domains [26]. The large domains result from high line tension due to a large hydrophobic thickness mismatch between the coexisting phases [34,62,63]. The linactant theory postulates that the addition of molecules that partition preferentially at domain interfaces should lower the line tension and result in smaller domains. This theory has gained more traction recently as Yang et al. showed that aToc can minimize line tension at domain boundaries as a means of protecting against HIV gp41-mediated membrane fusion [61].

In the case of α TocQ, the effect on lipid segregation is significantly less pronounced. In fact, there is an apparent increase in domain stability with even small amounts of α TocQ. Taken together, our results could lead to speculation of a physiological benefit for an effective membrane antioxidant. Phase boundaries have been identified as a favourable site for membrane permeation [64]. As suggested by Yang et al., tocopherol stabilizes domain interfaces to produce a less permeable boundary [61]. Considering the theory described by

Cruzeiro-Hansson and Mouritsen [65] and refined by Cordeiro [66], a reduction in bilayer thickness mismatch reduces the possibility of pore mediated permeation of oxidants. In the instance of membrane oxidation, the initial formation of hydroperoxide lipids promotes the formation of domain interfaces [67], which would be stabilized by the presence of tocopherols. As oxidation progresses, chemistry evolves the stable products α -tocopherylquinone and truncated lipids which together drives phase separation [68]. This final increase in lipid raft stability is a potential signal to recruit key proteins to recover or terminate the cell. In this manner, tocopherol would offer a new dimension to its antioxidant activity by protecting the cell membrane from oxidation induced lateral organization and permeation.

Again, we must be cautious in extending these observations into the physiological realm. The phase modulation we observe arises at vitamin E concentrations that have not been physiologically observed, even with extensive supplementation [11].

4. Conclusion

In an effort to begin testing a proposed mechanism of vitamin E's anti-cancer action, we reported on the effect that different members of the vitamin E family have on lipid domains. Data were collected using two different SANS configurations and microscopy, all of which yield consistent results with regards to vitamin E's influence on membrane organization. Though its phase behaviour is consistent with its membrane-protective role when in concentrations ranging between $0.0001 < \chi < 0.004$ [11], the lack of lipid domain response at $\chi = 0.02$ α Toc or γ Toc strongly suggests that increased vitamin E intake does not destabilize domains, as has been proposed. With regard to the complexity and variety of phase-active compounds in the native membrane, it seems unlikely that a local mole fraction of vitamin E greater than 0.02 is a definite actuator of domain stability. Therefore, the present work scrutinizes the validity of supplementing vitamin E as a presumed anti-cancer agent.

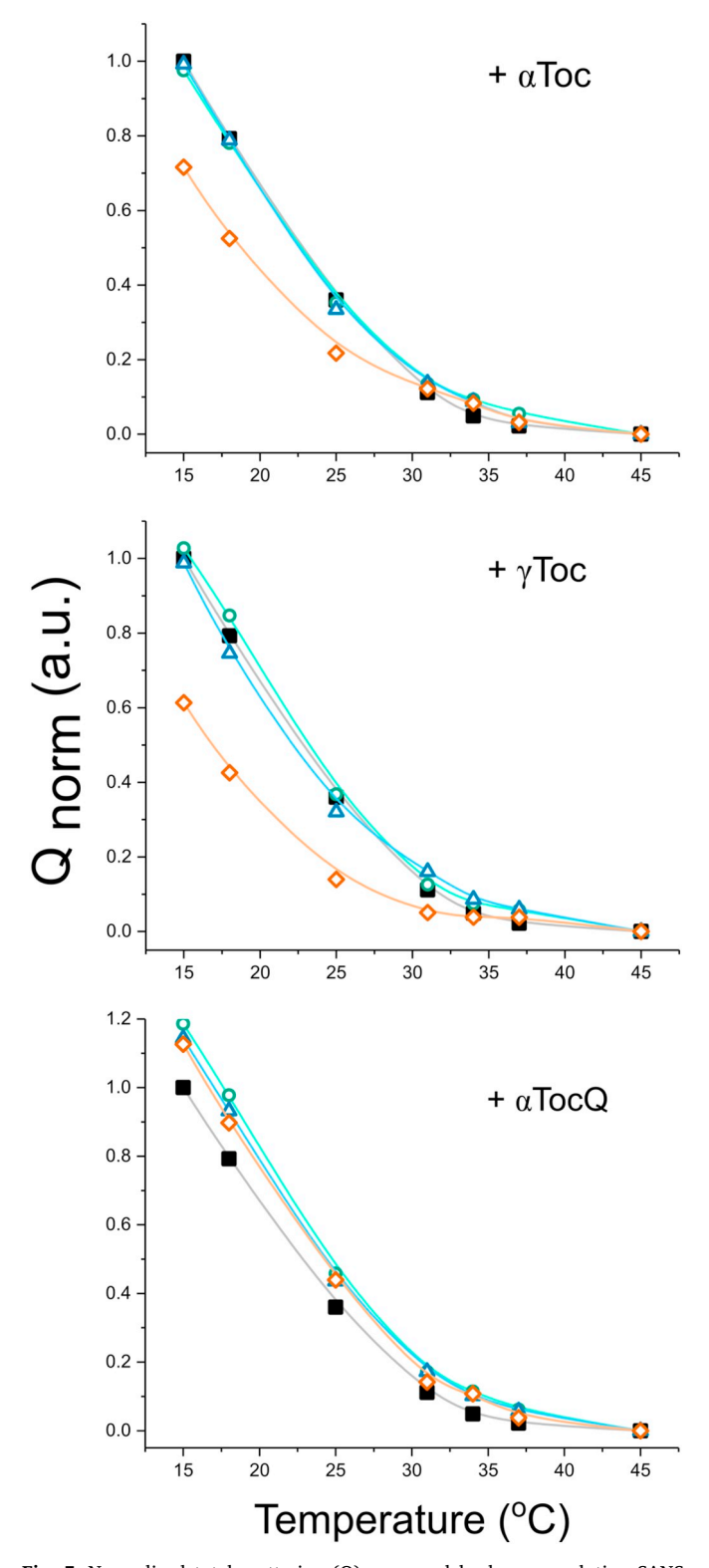


Fig. 5. Normalized total scattering (Q) measured by low q-resolution SANS. DPPC/DOPC/Chol samples containing $\chi=0$ (\blacksquare ; black), $\chi=0.02$ (\circ ; green), $\chi=0.05$ (\triangle ; blue) and $\chi=0.10$ (\Diamond , orange) of the vitamin E analogues α Toc (top), γ Toc (middle), and α TocQ (bottom). The mixtures were measured in the temperature range of 15–45 °C. Smooth curves were added to assist in visualizing trends in the data. Error is defined as one standard deviation and the error bars are smaller than the data markers.

Declaration of competing interest

The authors declare that they have no known competing financial interests or personal relationships that could have appeared to influence the work reported in this paper.

Acknowledgements

We acknowledge the support of the National Institute of Standards and Technology, U.S. Department of Commerce in providing access to the NG3 VSANS instrument through the Center for High Resolution Neutron Scattering, a partnership between the National Science Foundation and the National Institute of Standards and Technology under Agreement DMR-1508249. Certain commercial equipment or materials are identified in the paper to foster understanding. Such identification does not imply recommendation or endorsement by the National Institute of Standards and Technology, nor does it imply that the materials or equipment identified are necessarily the best available for the purpose. A portion of this research used resources from the CG3 BioSANS instrument at the High Flux Isotope Reactor, a DOE Office of Science User Facility operated by the Oak Ridge National Laboratory. J.K. is supported through the Scientific User Facilities Division of the Department of Energy Office of Science, sponsored by the Basic Energy Science Program, Department of Energy Office of Science, under contract number DEAC05-00OR22725. The authors thank Shuo Qian for his BioSANS technical assistance and Georg Pabst for access to the GAP program. F.A.H. acknowledges support from the National Science Foundation grant no. MCB-1817929. M.D., M.H.L.N. and B.W.R. are supported by Ontario Graduate Scholarships, D.M. acknowledges the support of the Natural Sciences and Engineering Research Council of Canada (NSERC), [funding reference number RGPIN-2018-04841] and the University of Windsor start-up funds.

Appendix A. Supplementary data

Supplementary data to this article can be found online at https://doi.org/10.1016/j.bbamem.2020.183189.

References

- H.M. Evans, K.S. Bishop, On the existence of a hitherto unrecognized dietary factor essential for reproduction, Science 56 (1922) 650–651.
- [2] R. Brigelius-Flohé, K.J. Davies, Is vitamin E an antioxidant, a regulator of signal transduction and gene expression, or a 'junk' food? Comments on the two accompanying papers: "Molecular mechanism of α-tocopherol action" by A. Azzi and "Vitamin E, antioxidant and nothing more" by M. Traber, Free Radical Biol. Med. 43 (2007) 2–3.
- [3] R. Brigelius-Flohé, Vitamin E: the shrew waiting to be tamed, Free Radical Biol. Med. 46 (2009) 543–554.
- [4] R. Brigelius-Flohé, F. Galli, Vitamin E: a vitamin still awaiting the detection of its biological function, Mol. Nutr. Food Res. 54 (2010) 583–587.
- [5] H.J. Kayden, M.G. Traber, Absorption, lipoprotein transport, and regulation of plasma concentrations of vitamin E in humans, J. Lipid Res. 34 (1993) 343–358.
- [6] M.G. Traber, Vitamin E Regulatory Mechanism, Annu. Rev. Nutr. 27 (2007) 347–362.
- [7] Dietary Reference Intakes for Vitamin C, Vitamin E, Selenium, and Carotenoids, 2000, 10.17226/9810.
- [8] M.G. Traber, J. Atkinson, Vitamin E, antioxidant and nothing more, Free Radical Biol. Med. 43 (2007) 4–15.
- [9] E. Niki, Role of vitamin E as a lipid-soluble peroxyl radical scavenger: in vitro and in vivo evidence, Free Radical Biol. Med. 66 (2014) 3–12.
- [10] K. Gohil, V.T. Vasu, C.E. Cross, Dietary α-tocopherol and neuromuscular health: search for optimal dose and molecular mechanisms continues!, Mol. Nutr. Food Res. 54 (2010) 693–709.
- [11] J. Atkinson, R.F. Epand, R.M. Epand, Tocopherols and tocotrienols in membranes: a critical review, Free Radical Biol. Med. 44 (2008) 739–764.

M. DiPasquale, et al. BBA - Biomembranes 1862 (2020) 183189

[12] H. Vatanparast, J.L. Adolphe, S.J. Whiting, Socio-economic status and vitamin/mineral supplement use in Canada. Health reports/Statistics Canada, Canadian Centre for Health Information, 21 2010, pp. 19–25.

- [13] E.A. Klein, I.M. Thompson, C.M. Tangen, J.J. Crowley, S. Lucia, P.J. Goodman, L.M. Minasian, L.G. Ford, H.L. Parnes, J.M. Gaziano, D.D. Karp, M.M. Lieber, P.J. Walther, L. Klotz, J.K. Parsons, J.L. Chin, A.K. Darke, S.M. Lippman, G.E. Goodman, F.L. Meyskens, L.H. Baker, Vitamin E and the risk of prostate cancer: the selenium and vitamin E cancer prevention trial (SELECT), JAMA, J. Am. Med. Assoc. 306 (2011) 1549-1556.
- [14] S.M. Lippman, E.A. Klein, P.J. Goodman, M.S. Lucia, I.M. Thompson, L.G. Ford, H.L. Parnes, L.M. Minasian, J.M. Gaziano, J.A. Hartline, J.K. Parsons, J.D. Bearden, E.D. Crawford, G.E. Goodman, J. Claudio, E. Winquist, E.D. Cook, D.D. Karp, P. Walther, M.M. Lieber, A.R. Kristal, A.K. Darke, K.B. Arnold, P.A. Ganz, R.M. Santella, D. Albanes, P.R. Taylor, J.L. Probstfield, T.J. Jagpal, J.J. Crowley, F.L. Meyskens, L.H. Baker, C.A. Coltman, Effect of selenium and Vitamin E on risk of prostate cancer and other cancers, Jama 301 (2009) 39.
- [15] Y.C. Li, M.J. Park, S.K. Ye, C.W. Kim, Y.N. Kim, Elevated levels of cholesterol-rich lipid rafts in cancer cells are correlated with apoptosis sensitivity induced by cholesterol-depleting agents, Am. J. Pathol. 168 (2006) 1107–1118.
- [16] K. Simons, M.J. Gerl, Revitalizing membrane rafts: new tools and insights, Nat. Rev. Mol. Cell Biol. 11 (2010) 688–699.
- [17] D. Lingwood, K. Simons, Lipid rafts as a membrane-organizing principle, Science 327 (2010) 46–50.
- [18] N. Resnik, U. Repnik, M.E. Kreft, K. Sepčić, P. Maček, B. Turk, P. Veranič, Highly selective anti-cancer activity of cholesterol-interacting agents methyl-β-cyclodextrin and Ostreolysin A/Pleurotolysin B protein complex on urothelial cancer cells, PLOS ONE 10 (2015) 1–19.
- [19] A. Badana, M. Chintala, G. Varikuti, N. Pudi, S. Kumari, V.R. Kappala, R.R. Malla, Lipid raft integrity is required for survival of triple negative breast cancer cells, J. Breast Cancer 19 (2016) 372–384.
- [20] C.S. Yang, N. Suh, A.N.T. Kong, Does vitamin E prevent or promote cancer? Cancer Prev. Res. 5 (2012) 701–705.
- [21] G.X. Li, M.J. Lee, A.B. Liu, Z. Yang, Y. Lin, W.J. Shih, C.S. Yang, δ-tocopherol is more active than α- or γ-tocopherol in inhibiting lung tumorigenesis in vivo, Cancer Prev. Res. 4 (2011) 404–413.
- [22] J. Ju, S.C. Picinich, Z. Yang, Y. Zhao, N. Suh, A.N. Kong, C.S. Yang, Cancer-preventive activities of tocopherols and tocotrienols, Carcinogenesis 31 (2010) 533–542.
- [23] C. Eggeling, C. Ringemann, R. Medda, G. Schwarzmann, K. Sandhoff, S. Polyakova, V.N. Belov, B. Hein, C. Von Middendorff, A. Schönle, S.W. Hell, Direct observation of the nanoscale dynamics of membrane lipids in a living cell, Nature 457 (2009) 1159–1162.
- [24] E.L. Elson, E. Fried, J.E. Dolbow, G.M. Genin, Phase separation in biological membranes: integration of theory and experiment, Annu. Rev. Biophys. 39 (2010) 207–226.
- [25] J.D. Nickels, S. Chatterjee, C.B. Stanley, S. Qian, X. Cheng, D.A.A. Myles, R.F. Standaert, J.G. Elkins, J. Katsaras, The in vivo structure of biological membranes and evidence for lipid domains, PLoS Biol. 15 (2017) 1–22.
- [26] G.W. Feigenson, Phase boundaries and biological membranes, Annu. Rev. Biophys. Biomol. Struct. 36 (2007) 63–77.
- [27] G.W. Feigenson, Phase diagrams and lipid domains in multicomponent lipid bilayer mixtures, BBA-Biomembranes 1788 (2009).
- [28] D. Marquardt, F.A. Heberle, J.D. Nickels, G. Pabst, J. Katsaras, On scattered waves and lipid domains: detecting membrane rafts with X-rays and neutrons, Soft Matter 11 (2015) 9055–9072.
- [29] G.W. Feigenson, J.T. Buboltz, Ternary phase diagram of dipalmitoyl-PC/dilauroyl-PC/cholesterol: nanoscopic domain formation driven by cholesterol, Biophys. J. 80 (2001) 2775–2788.
- [30] S.L. Veatch, S.L. Keller, Separation of liquid phases in giant vesicles of ternary mixtures of phospholipids and cholesterol, Biophys. J. 85 (2003) 3074–3083.
- [31] F.A. Heberle, G.W. Feigenson, Phase separation in lipid membranes, Cold Spring Harb. Perspect. Biol. 3 (2011) 1–13.
- [32] S.L. Veatch, S.L. Keller, Seeing spots: complex phase behavior in simple membranes, Biochim. Biophys. Acta, Mol. Cell Res. 1746 (2005) 172–185.
- [33] P. Heftberger, B. Kollmitzer, A.A. Rieder, H. Amenitsch, G. Pabst, In situ determination of structure and fluctuations of coexisting fluid membrane domains, Biophys. J. 108 (2015) 854–862.
- [34] F.A. Heberle, R.S. Petruzielo, J. Pan, P. Drazba, N. Kučerka, R.F. Standaert, G.W. Feigenson, J. Katsaras, Bilayer thickness mismatch controls raft size in model membranes, J. Am. Chem. Soc. 135 (2013) 6853–6859.
- [35] O. Arnold, J.C. Bilheux, J.M. Borreguero, A. Buts, S.I. Campbell, L. Chapon, M. Doucet, N. Draper, R. Ferraz Leal, M.A. Gigg, V.E. Lynch, A. Markvardsen, D.J. Mikkelson, R.L. Mikkelson, R. Miller, K. Palmen, P. Parker, G. Passos, T.G. Perring, P.F. Peterson, S. Ren, M.A. Reuter, A.T. Savici, J.W. Taylor, R.J. Taylor, R. Tolchenov, W. Zhou, J. Zikovsky, Mantid Data analysis and visualization package for neutron scattering and μ SR experiments, Nucl. Instrum. Methods Phys. Res., Sect. A 764 (2014) 156–166.
- [36] S.R. Kline, Reduction and analysis of SANS and USANS data using IGOR Pro, J. Appl. Crystallogr. 39 (2006) 895–900.
- [37] O. Glatter, O. Kratky, Chapter 2, Small Angle X-Ray Scattering, Academic Press, New York, 1982.
- [38] J. Pencer, V.N. Anghel, N. Kučerka, J. Katsaras, Scattering from laterally heterogeneous vesicles. I. Model-independent analysis, J. Appl. Crystallogr. 39 (2006) 791–796.

[39] P.V. Konarev, V.V. Volkov, A.V. Sokolova, M.H. Koch, D.I. Svergun, PRIMUS: a Windows PC-based system for small-angle scattering data analysis, J. Appl. Crystallogr. 36 (2003) 1277–1282.

- [40] G. Pabst, M. Rappolt, H. Amenitsch, P. Laggner, Structural information from \nmultilamellar liposomes at full hydration: full q-range fitting with high quality xray\ndata, Phys. Rev. E 52 (2000) 4000–4009.
- [41] G. Pabst, J. Katsaras, V.A. Raghunathan, M. Rappolt, Structure and interactions in the anomalous swelling regime of phospholipid bilayers, Langmuir 19 (2003) 1716–1722.
- [42] T.M. Konyakhina, G.W. Feigenson, Phase diagram of a polyunsaturated lipid mixture: brain sphingomyelin/1-stearoyl-2-docosahexaenoyl-sn-glycero-3-phosphocholine/chole sterol, BBA-Biomembranes 1858 (2016) 153–161.
- [43] M.I. Angelova, S. Soléau, P. Méléard, F. Faucon, P. Bothorel, Preparation of giant vesicles by external AC electric fields. Kinetics and applications. in: C. Helm, M. Lösche, H. Möhwald (Eds.), Trends in Colloid and Interface Science VI, Springer, 1992, pp. 127–131.
- [44] T. Baumgart, G. Hunt, E.R. Farkas, W.W. Webb, G. Feigenson, Fluorescence probe partitioning between Lo /Ld phases in lipid membranes, Biochim Biophys Acta. 1768 (2007) 2182–2194.
- [45] E. Baykal-Caglar, E. Hassan-Zadeh, B. Saremi, J. Huang, Preparation of giant unilamellar vesicles from damp lipid film for better lipid compositional uniformity, BBA-Biomembranes 1818 (2012) 2598–2604.
- [46] J. Heuvingh, S. Bonneau, Asymmetric oxidation of giant vesicles triggers curvatureassociated shape transition and permeabilization, Biophys. J. 97 (2009) 2904–2912.
- [47] P. Heftberger, B. Kollmitzer, F.A. Heberle, J. Pan, M. Rappolt, H. Amenitsch, N. Kučerka, J. Katsaras, G. Pabst, Global small-angle X-ray scattering data analysis for multilamellar vesicles: the evolution of the scattering density profile model, J. Appl. Crystallogr. 47 (2014) 173–180.
- [48] N. Kučerka, M.P. Nieh, J. Katsaras, Fluid phase lipid areas and bilayer thicknesses of commonly used phosphatidylcholines as a function of temperature, Biochim. Biophys. Acta, Biomembr. 1808 (2011) 2761–2771.
- [49] D. Marquardt, J.A. Williams, N. Kučerka, J. Atkinson, S.R. Wassall, J. Katsaras, T.A. Harroun, Tocopherol activity correlates with its location in a membrane: a new perspective on the antioxidant Vitamin E, J. Am. Chem. Soc. 135 (2013) 7523–7533.
- [50] D. Marquardt, J.A. Williams, J.J. Kinnun, N. Kučerka, J. Atkinson, S.R. Wassall, J. Katsaras, T.A. Harroun, Dimyristoyl Phosphatidylcholine: a remarkable exception to α -tocopherol's membrane presence, J. Am. Chem. Soc. 136 (2014) 203–210.
- [51] D. Marquardt, N. Kučerka, J. Katsaras, T.A. Harroun, α-Tocopherols location in membranes is not affected by their composition, Langmuir 31 (2015) 4464–4472.
- [52] F.A. Heberle, M. Doktorova, S.L. Goh, R.F. Standaert, J. Katsaras, G.W. Feigenson, Hybrid and nonhybrid lipids exert common effects on membrane raft size and morphology, J. Am. Chem. Soc. 135 (2013) 14932–14935.
- morphology, J. Am. Chem. Soc. 135 (2013) 14932–14935.

 [53] D. Bolmatov, W.T. McClintic, G. Taylor, C.B. Stanley, C. Do, C.P. Collier, Z. Leonenko, M.O. Lavrentovich, J. Katsaras, Deciphering melatonin-stabilized phase separation in phospholipid bilayers, Langmuir 35 (2019) 12236–12245.
- [54] K. Simons, J.L. Sampaio, Membrane organization and lipid rafts, (2011).
- [55] J.H. Lorent, B. Diaz-Rohrer, X. Lin, K. Spring, A.A. Gorfe, K.R. Levental, I. Levental, Structural determinants and functional consequences of protein affinity for membrane rafts. Nat. Commun. 8 (2017) 1219.
- [56] M. Schick, Membrane heterogeneity: manifestation of a curvature-induced microemulsion, Phys. Rev. E 85 (2012) 031902.
- [57] J.J. Amazon, S.L. Goh, G.W. Feigenson, Competition between line tension and curvature stabilizes modulated phase patterns on the surface of giant unilamellar vesicles: a simulation study, Phys. Rev. E 87 (2013) 022708.
- [58] S.L. Veatch, O. Soubias, S.L. Keller, K. Gawrisch, Critical fluctuations in domainforming lipid mixtures, Proc. Natl. Acad. Sci. 104 (2007) 17650–17655.
- [59] R. Brewster, P. Pincus, S. Safran, Hybrid lipids as a biological surface-active component, Biophys. J. 97 (2009) 1087–1094.
- [60] H.S. Muddana, H.H. Chiang, P.J. Butler, Tuning membrane phase separation using nonlipid amphiphiles, Biophys. J. 102 (2012) 489–497.
- [61] S.-T. Yang, V. Kiessling, L.K. Tamm, Line tension at lipid phase boundaries as driving force for HIV fusion peptide-mediated fusion, Nat. Commun. 7 (2016) 11401.
- [62] A.J. García-Sáez, S. Chiantia, P. Schwille, Effect of line tension on the lateral organization of lipid membranes, J. Biol. Chem. 282 (2007) 33537–33544.
- [63] J.D. Nickels, X. Cheng, B. Mostofian, C. Stanley, B. Lindner, F.A. Heberle, S. Perticaroli, M. Feygenson, T. Egami, R.F. Standaert, J.C. Smith, D.A. Myles, M. Ohl, J. Katsaras, Mechanical properties of nanoscopic lipid domains, J. Am. Chem. Soc. 137 (2015) 15772–15780.
- [64] D. Marsh, A. Watts, P.F. Knowles, Evidence for phase boundary lipid. Permeability of tempo-choline into dimyristoylphosphatidylcholine vesicles at the phase transition, Biochemistry 15 (1976) 3570–3578 pMID: 182212.
- [65] L. Cruzeiro-Hansson, O.G. Mouritsen, Passive ion permeability of lipid membranes modelled via lipid-domain interfacial area, BBA - Biomembranes 944 (1988) 63–72.
- [66] R.M. Cordeiro, Molecular structure and permeability at the interface between phase-separated membrane domains, J. Phys. Chem. B 122 (2018) 6954–6965.
- [67] T.M. Tsubone, H.C. Junqueira, M.S. Baptista, R. Itri, Contrasting roles of oxidized lipids in modulating membrane microdomains, Biochim. Biophys. Acta, Biomembr. 1861 (2019) 660–669.
- [68] R. Volinsky, R. Paananen, P.K.J. Kinnunen, Oxidized phosphatidylcholines promote phase separation of cholesterol-sphingomyelin domains, Biophys. J. 103 (2012) 247–254.